On Climate Change and Photovoltaic Energy Production

I. M. Peters, T. Buonassisi

Abstract:

As the 21st century progresses, photovoltaic technology is becoming a major provider of the world's electricity, while effects of global climate change unfold. This development begs the question: is climate change affecting the energy production of solar cells? In this article, we attempt to answer this question looking backward and forward. We start by analyzing recent trends for global meteorological conditions and solar cell performance parameters, covering the ten-year period between 20016 and 2015. We leverage a field-verified performance model for two of the most well-established solar cell technologies that also feature very different sensitivities to changing operating conditions: silicon and cadmium telluride. We find that climate change has already left its mark: ten years ago, silicon solar panels - on average - generated 4 kWh/m^2 more power than today. Correlating solar cell performance ratio changes and changes in operating conditions, we find that temperature globally is the leading factor for silicon (-0.52±0.03%/K), accounting for ~85% of the observed effect. Water related light absorption in the atmosphere is most likely responsible for much of the remaining contribution. To predict how future solar cell performance is affected, we focus on the implications of raising temperatures. For the end of the 21st century, we project that silicon PV panels globally will suffer performance reductions of between 0.7% and 2.5% (8 – 30 kWh/kWp in North America), depending on the global warming scenario. These reductions will result in significant socio-economic penalties, particularly in a world that produces a significant portion of its electricity from PV panels, and especially if additional effects of global warming, like accelerated panel degradation and extreme weather are considered. Mitigation strategies to reduce these losses include the extension of the electricity gird and the development of improved PV materials, as well as cell and module architectures.

Introduction:

Contemplating the 21st century, two developments seem likely: 1) the world will get warmer [1], and 2) solar panel deployment will increase [2-4]. Considering these developments in conjunction, the question arises: how will climate change affect photovoltaic (PV) energy production?

PV technology has seen tremendous improvements in every performance metric, including power conversion efficiencies [5], module costs, required energy and material for fabrication, or energy payback times [6]. These improvements have transformed solar cells from a curiosity into the most commonly installed new energy source in 2018 by capacity [7]. There is no reason to believe that this development is at an end, and continuous innovation will drive costs further down, reduce energy payback times even more, and enable deployment on the TW scale in the next years [8]. As PV electricity becomes a more important contributor to our energy infrastructure, effects that influence the power generation of PV installations become more important. It is well known that solar cell performance is affected by local meteorological. Solar cell operation is ruled by Boltzmann's statistics [9], resulting in a lower voltage output at higher temperatures. This effect is amplified by the temperature dependence of other mechanisms, such a recombination. The overall temperature dependence of a solar cell is described by its temperature power coefficient T_C, which ranges between -0.3%/K and -0.6%/K for today's silicon solar cells [10 -12]. Temperature is not the only relevant factor, though - water [13] and aerosols [14] in the atmosphere extinguish light and reduce the amount of current and voltage a solar cell can generated. Hence, the most well-established features of current climate change — rising temperatures and humidity [15] — will result in a reduction of the power output of any solar cell for fundamental reasons. The objective of this paper is to investigate and quantify the fundamental effects of climate change on solar cell performance in the past and in the future.

Several studies have addressed aspects of this problem, and provide clear indications that climate change needs to be considered for future PV energy production. Crook et al. [16] projected global energy yield for concentrating and non-concentrating PV installations based on results from the 4th assessment report of the Intergovernmental Panel on Climate Change (IPCC) [17] until 2080, using tabulated solar cell temperature and irradiance coefficients. They found small increase in yield in Europe and China, and decrease in the western USA and Saudi Arabia. Wild et al. [18] conducted a detailed analysis on temperature and insolation changes based on the 39 climate models used in the 5th assessment report of the IPCC [19]. Using the same models as Crook, they projected a declining energy yield in large parts of the world, but note exceptions for Europe, the South-East of North America and the South-East of China by 2049. The paper also discusses uncertainties and shows that for most regions trends in energy yield are not clear. Jerez et al. [20], evaluate the impact of climate change on PV power generation in Europe by 2080 and project relative reductions in power generation ranging from 1% for Spain to 12% in Scandinavia, with most regions laying between 2% and 5%. Bazyomo et al. [21] predicts decreasing power output in parts of Africa. Common to all these studies is the inclusion of predictions for trends in solar insolation. Following [18], variations in insolation are the biggest contributor to uncertainties in energy yield changes. These uncertainties can explain why there are inconsistencies for regional (though not for global) trends in between studies. Another aspect to consider is that, depending on when the study was conducted, results from the 4^{th} or 5^{th} IPCC assessment reports were used, and improvements in climate models made in between these reports need to be considered.

In addition to energy yield, performance ratio (*PR*) [22] is a common metric to assess PV installations. The advantage of *PR* is that it excludes insolation effects; we will use this metric in our projection of climate change induced losses. The impact of temperature on performance ratios globally was investigated, e.g. in [23]. However, no projections on temperature changes were considered. Regional impacts on

performance due to climate change were investigated by Bartos and Chester [24] for the Western United States. They predicted a 2% decrease in equivalent PV capacity between 2010 and 2060.

In this paper, we explore the impact of climate change on PV performance looking backwards, using past data and forwards, using projections. We leverage a detailed and field-verified PV performance model [25], and we consider two of the industrially most relevant PV technologies: silicon and cadmium telluride (CdTe). Silicon and CdTe were also chosen because they feature different band gaps, resulting in different sensitivities to temperature, water and aerosols [25], and allowing to demonstrate the role that technology can play. The focus of this paper is on the fundamental effect of climate change on solar cells, and we exclude system aspects.

Box I: *Sensitivities of Si and CdTe to operating conditions*

Silicon solar cells are far more sensitive to changes in operating conditions than those made of CdTe. One reason is the different band gap. The band gap of Si is with 1.12 eV much smaller than that of CdTe with 1.54eV. With respect to temperature, a smaller band gap is for fundamental reasons linked to a greater temperature coefficient [26], yet there is a technological component to it as well. Silicon solar cell with higher open-circuit voltage generally feature smaller temperature coefficients [27]. The temperature coefficient for CdTe used in this work is -0.26%/K [28], whereas the one for silicon is -0.45%/K [29]. The band gap also defines the range in which the two solar cell technologies absorb light. Silicon is active up to about 1150 nm wavelength, whereas CdTe only absorbs light with a wavelength smaller than about 850 nm. Water related light extinction predominantly occurs in the infrared part of the spectrum, and is more relevant for Si. Aerosol extinction affects the blue part of the spectrum more and, while reducing the current for both solar cells similarly, has a larger relative effect on CdTe. For a more detailed discussion of this topic, the reader is referred to [25] and [30].

We start by analyzing historic trends using global meteorological data from NASA covering the ten-year period between 2006 and 2015. Correlating solar cell performance trends to recent climatic trends, we establish quantitative relations of how climate change has affected different solar cell performance metrics in the recent past, highlighting the roles of temperature and humidity.

Using past results, we project how the global energy production of PV installations of the two considered technologies will be affected by climate change until 2100, using projections from IPCC's 5th assessment report and considering three detailed PV deployment scenarios. In our projections we focus on temperature predictions. This choice was motivated by the large uncertainties in projected local insolation changes and by the finding that temperature is the leading contributor to *PR* changes. Yet climate change is more complex than just global warming. Analysis of past data reveals the correlations between temperature, humidity and aerosols in the recent past, and we use these correlations in our projections. Locally, variations in insolation may have a stronger effect on energy production, but these effects are additive to the performance changes discussed here, and on a global average basis, no strong variations in total solar irradiance are projected until 2100 [31].

In the final part of the paper, we discuss consequences of our results as they pertain to a reduction in PV electricity output, additional detrimental effects of global warming, such as accelerated degradation, the potential benefits of using different PV technologies, and mitigation strategies such as extensions of the electricity grid.

Method:

To estimate how climate change affects the performance of different solar cells, we perform the procedure outlined in **Figure 1**, which consists of four steps.

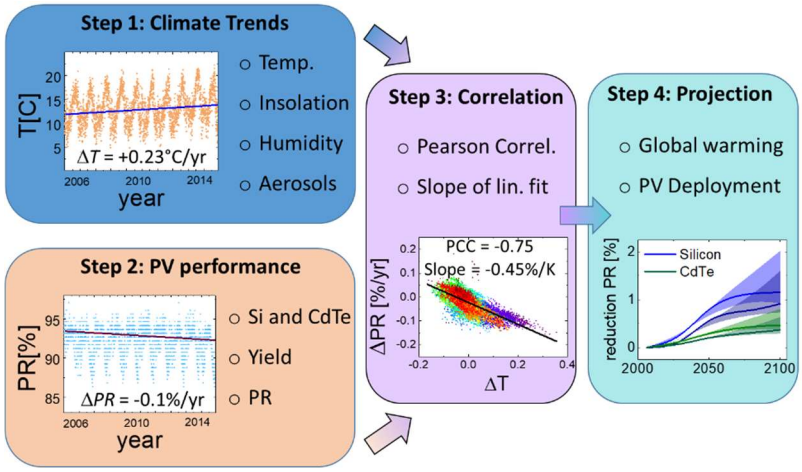

Figure 1: *Schematic of the adopted approach to estimate the impact of climate change on PV performance reduction. In step 1 ten-year time series of meteorological parameters are analyzed and trends are identified. In step 2 the same is done for Photovoltaic performance parameters. The trends are established everywhere on the planet and correlations between trends are established in step 3. Finally, correlations between solar cell performance and temperature are used to project global performance reductions in the year 2100 in step 4.*

Step1: we analyzed time series of relevant meteorological parameters globally during the ten-year time period from 2006 to 2015. Parameters considered include insolation $I(t)$, temperature $T(t)$, precipitable water $TPW(t)$ and aerosol optical depth $AOD(t)$ These data were obtained from [32-35]. Trends for insolation and temperature were obtained through linear fits, with the annual change rates denoted ΔI, ΔT, ΔTPW and ΔAOD. Precipitable water and aerosols affect solar cells by reducing light transmission through the atmosphere. Changes in light transmission were calculated by

$$\Delta T_{TPW} = T\left[\left(TPW_{mean} + \frac{\Delta TPW}{2}\right)\right] - T\left[\left(TPW_{mean} - \frac{\Delta TPW}{2}\right)\right] \quad (1)$$

$$\Delta T_{AOD} = Exp\left[-AOD_{mean} + \frac{\Delta AO}{2}\right] - Exp\left[-AOD_{mean} - \frac{\Delta AOD}{2}\right] \quad (2)$$

And are denoted ΔT_{TPW} and ΔT_{AOD}. $T[TPW]$ is the water dependent light transmission of the solar spectrum through the atmosphere for a given value of total precipitable water as calculated using SMARTS

[36, 37]. The reference point of 100% transmission is set at a TPW value of 0. The calculations require specifying a wavelength range, as baseline, we use the range relevant to silicon solar cells (300 nm to 1150 nm). Other conditions are chosen to approximate the AM1.5 spectrum as closely as possible. Data for AOD is given for a wavelength of 550 nm. Results are shown in **Figure 2** and are discussed in the next section (*Step 1: Trends in relevant meteorological conditions*).

Step 2: we used field-test verified PV performance models [25] to calculated energy yield (*yield*) and performance ratio (*PR*) for a silicon and a CdTe solar cells. The energy yield of a solar cell specifies the total amount of energy delivered by it over a certain time and is given by

$$yield(t) = \int dt\, P_{out}(t) = \int dt\, d\lambda\, I(t) \cdot \eta(I, T, TPW, AOD, \lambda) \quad (3)$$

with P_{out} the output power of the solar cell at any given instant. Output power can be calculated as the product of measured insolation $I(t)$ and the solar cell conversion efficiency η. Efficiency depends on all meteorological factors and is calculated using methods described in [13] and [25]. Note that this calculation considers spectral effects through efficiency. Performance ratio specifies the output of a solar cell with respect to a chosen reference value. In this work, the reference value is the standard testing condition (STC) efficiency of the solar cell η_{STC} [27], and performance ratio is defined as:

$$PR(t) = \frac{yield}{\int dt\, I(t) \cdot \eta_{STC}} \quad (4)$$

Similarly as with meteorological factors, trends were obtained by linear fit and annual changing rates are denoted Δ*yield* and Δ*PR*. The two solar cell technologies Si and CdTe were chosen because they represent over 97% of current PV manufacturing capacity [39], and because of their difference in band gap. According to a previous study [13], we expect that materials with different band gaps are affected differently by climate change. Trends in solar cell performance metrics are shown in **Figures 3a - d** and **4a** - **d,** and are discussed in section *Step 2: Trends in Energy Yield and Performance Ratio*.

Step 3: we analyzed correlations between Δ*yield*, Δ*PR* and ΔI, ΔT, ΔT_{TPW} and ΔT_{AOD}. We use a cluster analysis to classify regions with different climate change characteristics, and correlations were analyzed

based on clusters and combined data sets. Pearson Correlation Coefficients [40] were used to determine the strength of a correlations. All significant correlations are discussed in section *Step3: Correlations*. A linear fit can be interpreted as a first-order approximation of the unknown, true correlation and can be used to established implied first-order coefficient. In all cases, the data did not support significant higher-order contributions. This analysis reveals quantitatively how solar cell performance ratio and energy yield are affected by changes in climate. Results are shown in **Figures 6** through **9**.

Step 4: we use the obtained correlations to project how energy production by different solar cells is affected by global warming in different climate scenarios. We use climate scenarios and data from the 5th IPCC report [19]. In addition, we make assumptions about future deployment scenarios. The results of this final step are discussed in section *Projection onto IPCC scenarios* and are displayed in **Figures 10** and **11**.

Step 1: Trends in relevant meteorological conditions.

Results for Step 1, analyzing ten-year time series of meteorological data and identifying trends, are shown in **Figure 2**. The results of the depicted figures are the annual changes derived through linear fitting. Insolation data (**Figure 2 a**) was taken from NASA's Clouds and Earth's Radiant Energy System (CERES) [32] satellite instrument. Surface air temperature (**Figure 2 b**), relative surface humidity and total precipitable water data (**Figure 2 c**) were taken from NASA's Atmospheric InfraRed Sounder (AIRS) instrument from the Earth Observing System (EOS) [33]. Aerosol parameters: single scattering albedo, optical depth (**Figure 2d),** and angstrom parameter, as well as ground reflectance data (not shown) were taken from NASA's Ozone Monitoring Instrument (OMI) [34], and from NASA's Moderate Resolution Imaging Spectroradiometer (MODIS) [35].

a) annual change in insolation

b) annual change in temperature

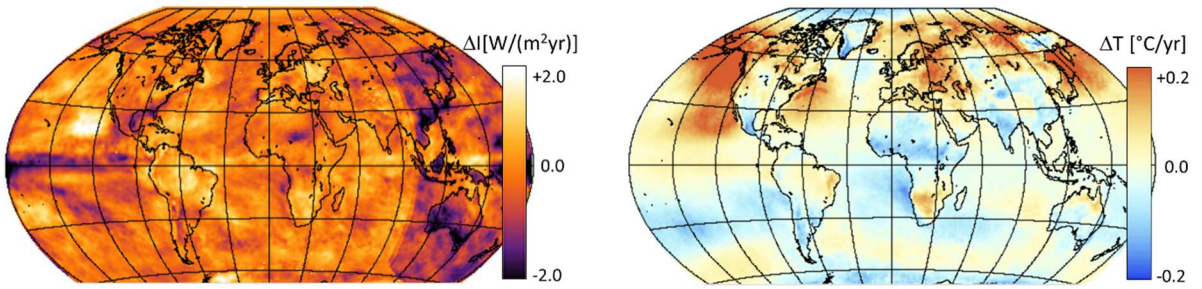

c) annual change in TPW light transmission (T_{TPW})

d) annual change in AOD light transmission (T_{AOD})

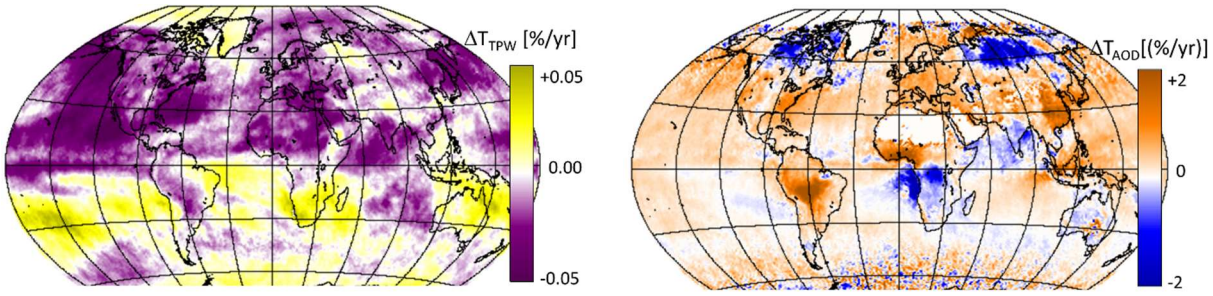

Figure 2: *Maps of the average annual changes in insolation ΔI (a), temperature ΔT (b), precipitable water related light transmission ΔT_{TPW} (c) and aerosol related light transmission ΔT_{AOD} (d) based on linear fitting over a ten-year time period (2006 to 2015). Sample size: 236,520,000 data points were used for each plot.*

Regarding Insolation data (ΔI, **Figure 2a**), we observe a systematically higher reduction in insolation in an area east of 100° E, which we believe to be an artefact. One indication is the shape of the affected area, which is almost rectangular in the cylindrical projection. The reduction is not obvious from any of the insolation time series in the affected area, but when plotting trends, the darker hue is obvious. On average, values for insolation changes are about 0.8 W/(m^2·yr) lower than in the remaining area. In the remaining work, we have excluded the area east of 100° E for all analyses using insolation trends.

With respect to temperature trends (**Figure 2b**), we find that our analysis generally agrees with studies published by NASA, for example [41, 42]. In line with [42], we find an overall warming rate of 0.02 K/year

for the whole planet. Temperature changes correlate weakly with changes in insolation (i.e. there is a trend that places that get sunnier also get hotter), and correlates in a cross pattern with change in total precipitable water (i.e. there are places that get hotter and drier, and other places get hotter and more humid). Correlations and average global trends are shown in the supporting material.

Please note that most studies that investigate global warming are done over much longer time periods. The ten-year trends shown here are at best weak indicators for local temperature developments. Regions in blue, indicating a temperature reduction in the last ten years, are no indication for an overall cooling as temperatures have steadily risen over the past 100 years [43]. This work is concerned with exploring how changes in temperature correlate with changes in PV performance, a ten-year period is sufficient to identify trends and establish these correlations.

There are many contributors to changes in insolation, including for example sun activity [44] and clouds [45]. Two additional contributors are light extinction through precipitable water and aerosols. We have investigated these aspects separately, using satellite data on *AOD* and *TPW* and equations 1 and 2. The results are shown in **Figure 2 c** and **d**. Overall, we find an increase in humidity resulting in reduced water related light transmission (T_{TPW}) for most of the Northern hemisphere and big parts of the landmass in the Southern Hemisphere. Light transmission here is calculated for a spectral range of 300 to 1150 nm wavelength. The analysis for aerosol related light transmission (T_{AOD}) creates a more diverse picture with the majority of the land mass experiencing an increase in transmission. Note that the scale for aerosol light transmission is valid only for a single wavelength (550 nm); the effect on the overall light intensity is much smaller and depends on the considered spectral range as well as the Angstrom Exponent. The contribution of aerosols changes is the most difficult to quantify.

Step 2: Trends in Energy Yield and Performance Ratio.

In step 2 we use established global solar cell performance models [25] to determine trends in key performance characteristics — yield and performance ratio — of two solar cell technologies — Si and CdTe.

I Energy Yield

In a first series of calculations, we computed annual changes in energy yield (Δ_{yield}) and analyzed statistical distributions. These calculations require an assumption about the distribution of solar panels. In the results discussed here, we use the PV everywhere scenario (described in Step 4). Results are shown in Figure 3. Energy yield is proportional to insolation, and we observe the same artefact in yield changes (**Figures 3a** and **b**) as in insolation changes (compare **Figure 2a**). The affected area was excluded for the analysis. Overall, the developments in yield look similar for Si and CdTe: Yield increases in South America, South Africa and parts of Europe, decreases in northern Africa and North America. When looking at the overall distribution of yield values over the entire land mass (**Figures 3c** and **d**), we find that energy yield on average decreased by 0.4 kWh/(m^2·yr) for silicon and by 0.1 kWh/(m^2·yr) for CdTe. Note that we did not consider the actual distribution of solar installations. We will discuss this in the section on projections to IPCC scenarios.

a) Silicon

b) Cadmium Telluride

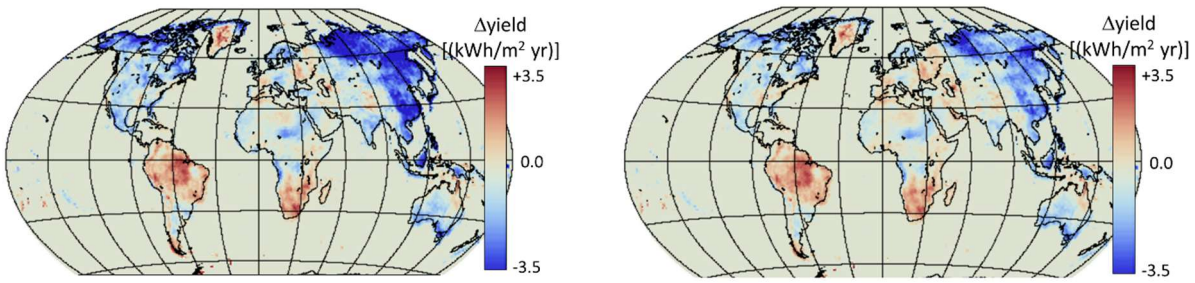

c) statistical distribution Si

d) statistical distribution CdTe

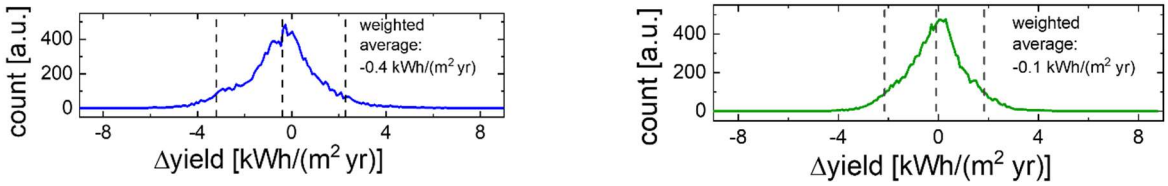

Figure 3: *Global annual average energy yield changes between 2006 and 2015 for silicon (a) and CdTe (b). Statistical distribution of yield changes, excluding data east of 100°E due to the artifacts in insolation data — see previous section (c and d). Colors indicate latitudes. Sample size in each plot: 12,878.*

II Performance Ratio

In a second series of calculations, we computed the distribution and statistical properties of performance ratios (*PR*) of the two solar cell technologies (**Figure 4**). The advantage of *PR* is that it is independent of insolation and efficiency, and excludes both of these factors. Excluding insolation eliminates the artefacts seen in **Figure 2a** and allows analyzing data across the entire globe.

When looking at the changes in *PR* (Δ*PR*), the differences between the two PV technologies become apparent (**Figure 4a** and **b**). Whereas silicon shows an overall decrease in *PR* almost everywhere on the planet (with exceptions in Central Africa, South America, Central Asia and southern Australia), the picture is more diverse for CdTe, which shows increasing *PR*s in some areas and decreases in others. This qualitative picture is confirmed when looking at the statistical distributions (**Figure 4c** and **d**). *PR*s for silicon decreased on average by 0.4% annually over the investigated period, whereas for CdTe we observe

a very small increase of 0.025% on average annually. An increasing *PR* is not contradictory to a decreasing yield, the reason lies in the way that *PR* is calculated, as we will show later.

a) Silicon

b) Cadmium Telluride

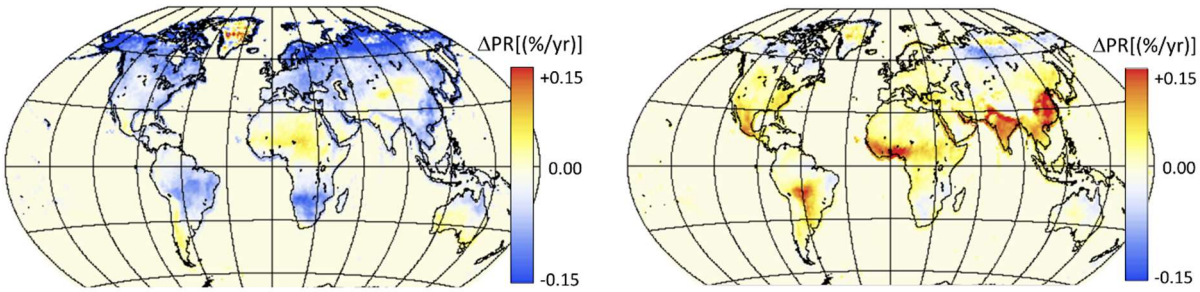

c) statistical distribution Si

d) statistical distribution CdTe

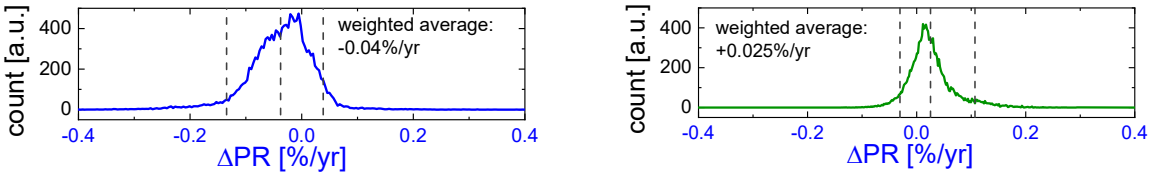

Figure 4: *Global annual average performance ratio changes over the period 2006 to 2015 for silicon (a) and CdTe (b). Statistical distribution of performance ratio changes (c and d). Sample size in each plot: 12,878.*

Step 3: Correlations.

In this step we investigate how the trends in meteorological conditions and solar cell performance correlate. Cluster analysis is used to identify regions with different climate trend characteristics, and the impact of climate change on solar cell energy yield and performance ratios are quantified.

I Cluster Analysis

One challenge in this study was that there are a number of counteracting trends in the development of meteorological conditions over the past ten years. One example can be made visible by plotting the

temperature anomaly versus the anomaly in humidity (Figure 5a). The figure shows a cross pattern with both positive and negative correlations between these two factors. The underlying physical processes are that hotter air has a higher absolute humidity capacity, but can at the same time cause an area to become drier. These overlying trends can result in a Simpson's paradox [46] when analyzing the impact on solar cells. To avoid this situation, we have used the Neighborhood Contraction clustering method [47]. This approach determines the number of present clusters automatically. The six resulting clusters are plotted in **Figure 5a**, and can be interpreted in a meaningful way. Cluster 1 describes areas that have seen little changes in precipitable water or temperature in the last ten years (neutral cluster, green). Cluster 2 describes areas that have gone warmer. This cluster also shows a slightly positive correlation between temperature and precipitable water (hot cluster, red). Cluster 3 describes areas that have gone drier without temperature changing much (dry cluster, dark yellow). Cluster 4 describes areas that have become more humid without temperature changing much (humid cluster, light blue). Cluster 5 describes areas that have become more humid and colder (cold + humid cluster, dark blue). Cluster 6 describes areas that have become warmer and drier (hot + dry cluster, orange). Also, in cluster 5 and 6 show a positive correlation between precipitable water and temperature. The described color code will be used throughout the following analysis. In Figure 5b, we show where in the world the different clusters are located.

a) cluster analysis

b) global distribution of clusters

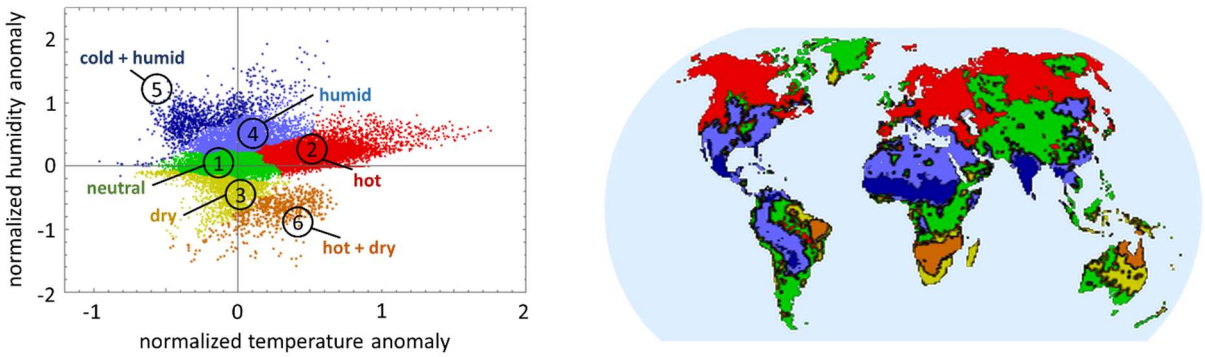

Figure 5: *Cluster analysis of temperature and humidity anomaly (a). Six clusters were identified that can be interpreted as recent climate trends. Cluster 1 (neutral) contains 10,819 data points, cluster 2 (hot) 7,795, cluster 3 (dry) 1,566, cluster 4 (humid) 3,390, cluster 5 (cold + humid) 1,125 and cluster 6 (hot + dry) 582. The global distribution of these clusters is shown in (b).*

II Solar Cell Performance

A number of correlations between recent climate trends and changes in solar cell performance can be observed. In the following we summarize and discuss the role of the different meteorological factors on solar cell yield and performance ratio.

a) The role of insolation changes

Insolation directly scales energy yield. Hence, a linear correlation between Δyield and ΔI is expected and is observed for both investigated solar cell technologies (**Figure 6**). An implied solar cell efficiency can be calculated from the slope through division by the number of hours per year (8760); this operation transforms yield (kWh) into an average power (kW). The obtained values, 20.5 ± 1% for silicon and 17.5 ± 1% for CdTe agree with the actual efficiencies of the considered solar cells (21.3% and 17.3%). This agreement can be considered a sanity check for the presented method. It is also a first example for the usefulness of the clustering method. Lateral shifts between the clusters result in an overestimation of the

implied efficiency if the data is analyzed without prior processing. Elevated temperatures actually *reduce* the solar cell efficiency. This effect is correctly captured by the cluster analysis, and is most obvious for the "hot" cluster in silicon, the material with the higher sensitivity to temperature changes. The discrepancy between actual and implied efficiency for silicon can also be attributed mostly to temperature effects (see next section).

a) Silicon

b) CdTe

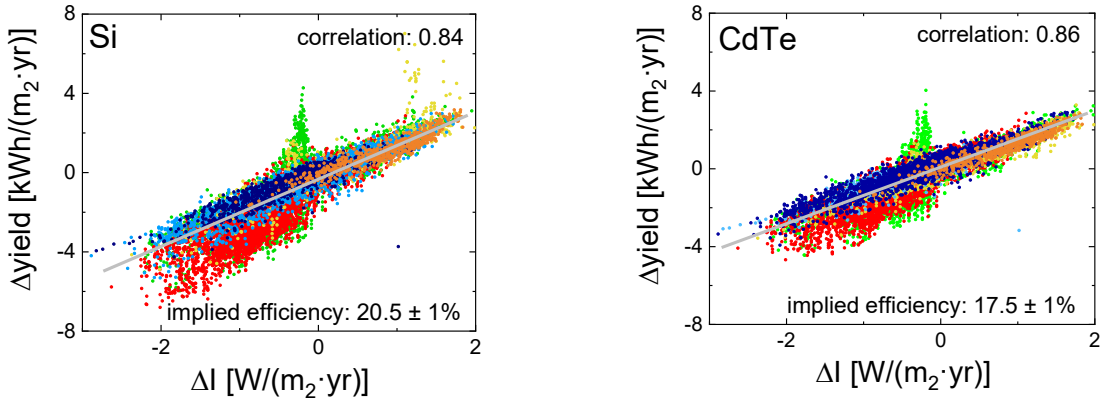

Figure 6: *Yield changes plotted against changes in insolation for Si (a) and CdTe (b). Color coding indicates the different clusters. The shown linear fit is the weighted average of the fits for the different clusters. The slope can be translated into an implied efficiency. The actual solar cell efficiencies are 21.3% (silicon) and 17.3% (CdTe). Sample sizes are specified in Figure 5.*

b) The role of temperature changes

Temperature affects voltage, current and the resistivities of a solar cell [48], with lower band gap materials like silicon being more sensitive than larger band gap materials like CdTe. While it is well established that elevated temperatures reduce the power output of any solar cell, the investigated temperature changes did not produce a clear signature on energy yield directly, due to the dominant role and overarching influence of insolation. For this reason, the role of temperature was explored for changes in performance

ratio (ΔPR), which excludes insolation effects. Results are shown in **Figure 7**. The data for each cluster was fitted linearly (details shown in the supporting material), and the weighted average linear fit for all clusters is also shown in the figure. The highest correlations are obtained for the "hot + dry", the "humid" and the "cold + humid" clusters. Similarly, to the implied efficiency, the slope of this fit can be interpreted as an implied temperature coefficient (T_C). The obtained values are -0.52 ± 0.03%/K for Silicon and -0.1 ± 0.1%/K for CdTe. These values differ from the tabulated values, in case of silicon with -0.45%/K slightly and in case of CdTe with -0.26%/K notably. These differences indicate that, at least for silicon, temperature is the leading effect for changes in performance ratio, and accounts for ~85% of the observed change in yield and performance ratio shown in **Figure 4**. It also indicates that temperature is not solely responsible, and that 15% of the change is caused by something else. A possible candidate is precipitable water, which we will discuss in the next section.

For CdTe the picture is much less clear. At this point there appears to be a discrepancy between the tabulated and implied temperature coefficient that is not easily explainable. In the next section we will argue that at least some of this discrepancy can be explained by the way that PR is calculated, and that the influence of precipitable water and possibly aerosols must be considered to understand the results.

a) Silicon

b) CdTe

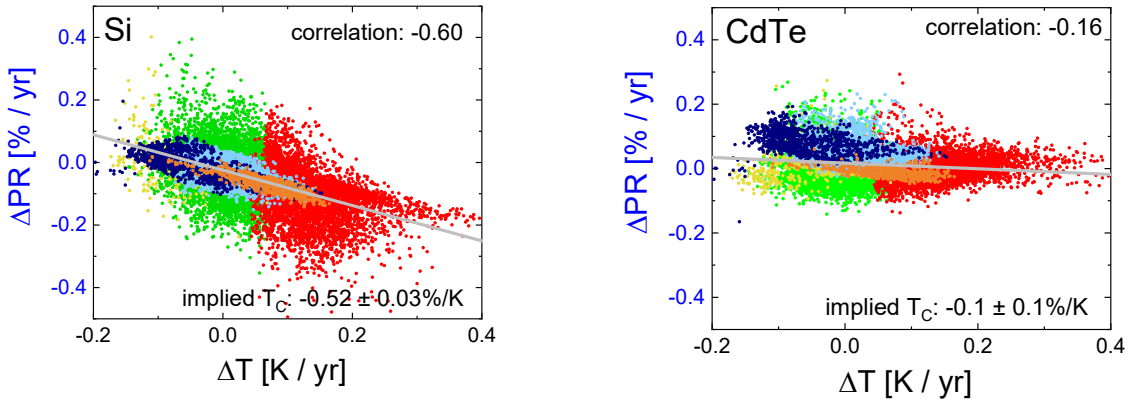

Figure 7: *ΔPR plotted against changes in temperature for Silicon (a) and CdTe (b). Color coding indicates the different clusters. The shown linear fit is the weighted average of the fits for the different clusters. The slope can be translated into an implied temperature coefficient T_C. The tabulated temperature coefficients are -0.45%/K (silicon) and -0.26%/K (CdTe). Sample sizes are specified in Figure 5.*

c) The role of precipitable water changes

Precipitable water absorbs sunlight on its path through the atmosphere. Consequently, it reduces light intensity and can be expected to reduce yield. A reduction in yield can be detected for silicon, when plotting changes in water related light transmission (ΔT_{TPW}) against *Δyield* with moderate significance (R_P = 0.28), as shown in **Figure 8a**. A positive correlation indicates that yield increases with transmission, which conforms to expectations. For CdTe no significant impact on yield was found (not shown).

The situation for performance ratio is different and less intuitive. It also differs for the different solar cell technologies. When investigating dependencies, we found that *ΔPR* and ΔT_{TPW} for CdTe exhibit a negative correlation with moderate significance (R_P = -0.39), whereas no significant correlation was found for silicon (not shown). This result may seem counter-intuitive but can be understood when considering the spectral ranges used in the calculations. When calculating ΔT_{TPW}, and yield we consider spectral effects up

to 1500 nm wavelength explicitly. This includes the active ranges for silicon (300 – 1150nm) nm and CdTe (300 - 850) nm. However, when calculating the reference yield (denominator in equation 4), the measured flux of the solar spectrum is used for insolation $I(t)$. The measured flux includes the infrared portion of the spectrum up to 4000 nm wavelength. As much of the precipitable water absorption happens within the infrared range, the relative reduction in reference yield is different from that of solar cell yield. Much of the water absorption happens outside the active range of CdTe. Consequently, the reference yield is reduced more proportionally than solar cell yield, resulting in the observed increase in PR with reduced light transmission ΔT_{TPW}. This is a quirk of the way *PR* is calculated, and does not mean that the solar cell becomes more efficient as light transmission is reduced. This behavior can also at least partially explain the discrepancy between the implied and tabulated temperature coefficient for CdTe in **Figure 7b** as ΔT and ΔT_{TPW} are moderately anti-correlated (R_P = -0.4). In the remaining manuscript, we will use tabulated values for CdTe behavior to avoid misinterpretations from the distortion.

Box II: An excurse into the pitfalls of history

At this point we must conclude that the results for CdTe are distorted. There are underlying reasons for why this is the case, that - we feel - warrant a short excurse. One reason is physical; silicon absorbs a wider range of the spectrum than CdTe, and hence changes in the spectrum always affect the balance between the active spectrum and the total spectrum for silicon less than for CdTe. A second possible reason is historical. Many of the tools for solar cell simulation were developed for silicon technology. Hence, using default settings will generate results that are best suited to understand and interpret the behavior of silicon solar cells. Throughout this study, the results for silicon are much easier to understand than those for CdTe and it requires a deeper look into spectral signatures to come to a coherent picture. This result should serve as a reminder that the introduction of any new technology will have unexpected consequences.

For silicon, much of the water related light absorption happens within its active spectral range, which includes ~95% of the insolation for which spectral effects are considered. Hence, solar cell yield and reference yield are affected similarly, resulting in the lack of a signature (The distortion resulting from this effect is approx. six times stronger for CdTe than for Si). To further explore the possible impact of ΔT_{TPW} on the implied temperature coefficient for silicon, we produced a subset of all conditions in which the humidity anomaly was close to zero (below 0.05 absolute value in **Figure 5**). In this subset the role of precipitable water changes is close to eliminated (plots shown in the supporting material). Recalculating the implied temperature coefficient resulted in a value of -0.48 ± 0.06%/K, indicating that precipitable water effects could also explain the higher value of the implied temperature coefficient for silicon.

a) yield silicon

b) performance ratio CdTe

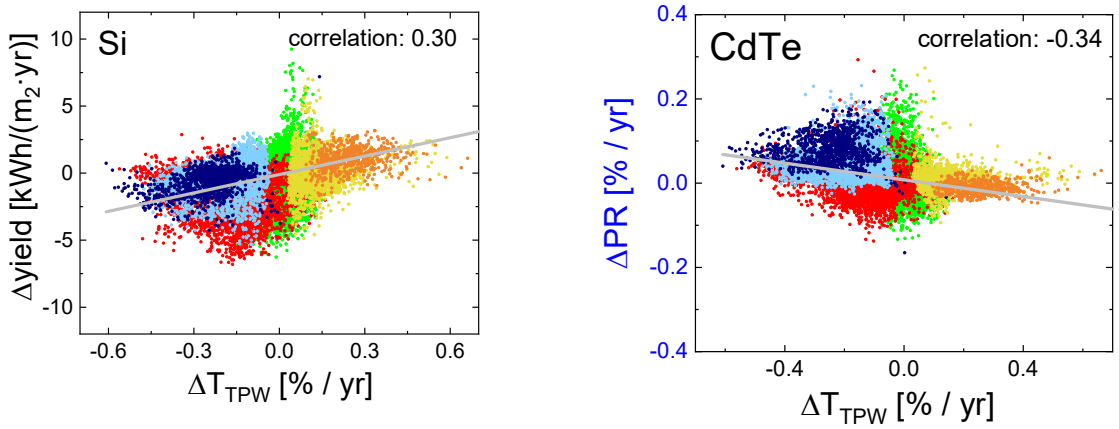

Figure 8: *Signatures of water related light transmission (ΔT_{TPW}) on the energy yield of Silicon (a) and the performance ratio of CdTe (2). Color coding indicates the different clusters. Linear fits of the combined data are shown as a guide to the eye. Sample sizes are specified in Figure 5.*

d) The role of aerosol changes

Aerosols affect solar cell performance in a similar way as precipitable water. They absorb or scatter light and, hence, reduce transmission through the atmosphere. A major difference is the spectral signature of aerosol related light extinction. While water predominantly absorbs infrared light, aerosols are more active in the visible part of the spectrum. As a consequence, they affect CdTe stronger than Si as CdTe obtains a relatively larger portion of its energy from visible light.

The impact of aerosol changes on solar cell performance is in many cases less significant than that of temperature and water, and it is more difficult to detect its signature. In addition, the used AOD data was more scattered, with gaps for certain regions and times (see **Figure 2d**). When exploring dependencies, we only found one dataset that showed a statistically significant correlation with ΔT_{AOD}: ΔPR of CdTe (**Figure 9**). Here, we find a positive correlation with moderate significance (R_P = 0.44) which conforms to expectations – higher aerosol levels should reduce performance. Yet, as mentioned for precipitable water, ΔPR must be interpreted considering spectral effects. But, also here, the explanation is straightforward: the majority of aerosol absorption happens within the spectral range in which CdTe is active. As this range only includes ~70% of the insolation for which spectral effects are considered, CdTe yield is now proportionally more affected than the reference yield, resulting in the observed positive correlation between ΔT_{AOD} and ΔPR.

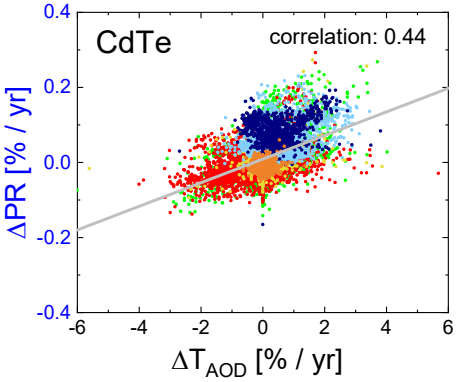

Figure 9: *Signature of aerosol related light transmission ΔT_{AOD} on changes in performance ratio ΔPR for CdTe. Colors indicate clusters, a linear fit for the combined data is added as a guide to the eye. Sample sizes are specified in Figure 5.*

Step 4: Projections.

The fourth and final step is a projection of how climate change will affect generation of PV electricity over the coming decades. We use the established correlations between trends in PV performance metrics and meteorological parameters, and project them onto climate scenarios as devised by the 5th assessment report of the IPCC [19]. Global warming projections according to the Representative Concentration Pathway (RCP) 4.5 scenario [49] and using NASAs bias correcting climate model [50] until 2100 are shown in **Figure 10a**.

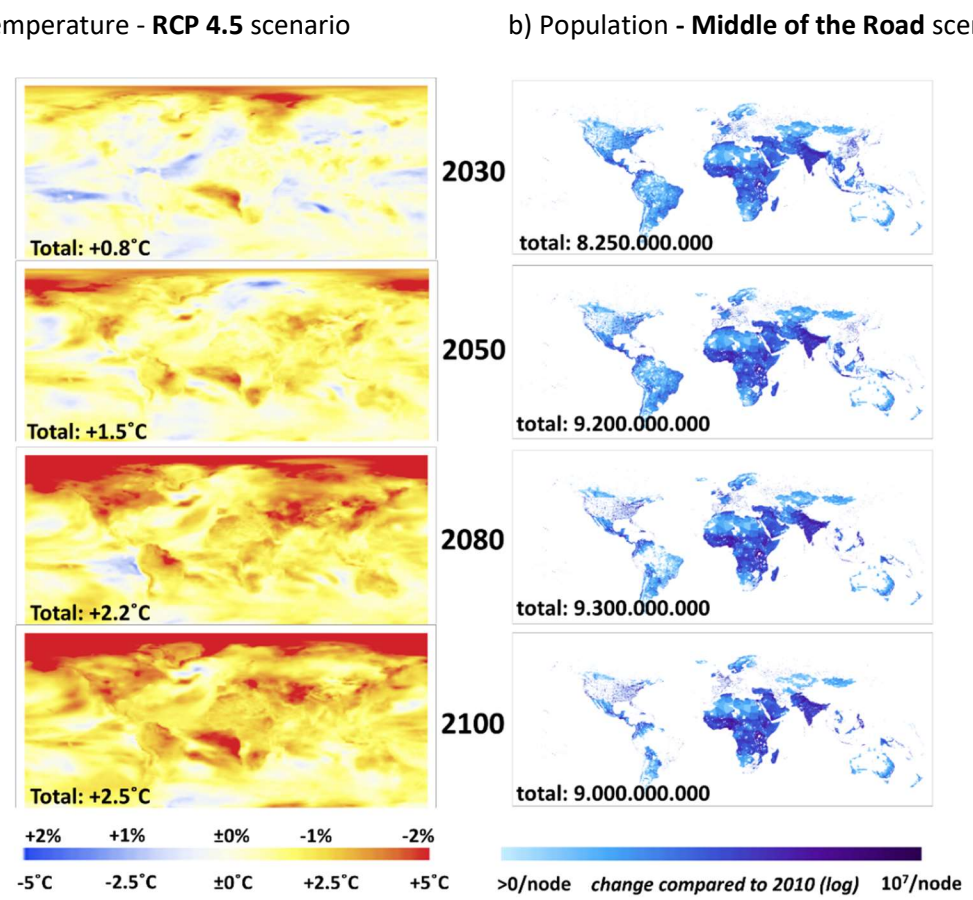

Figure 10: *Global warming according to the RCP 4.5 scenario of the IPCC [49] (a). Color indicates temperature changes, as shown on the lower scale, as well as PV performance changes, due to the used linear relation between the two. The upper axis indicates the performance change for silicon. Population*

development according to the Middle of the Road scenario [51, 52] is shown in (b) with projections for 2030, 2050, 2080 and 2100. Note that the depiction of population development was prepared for visual ease. The graph shows differences in population density compared to 2010 values on a log scale where any negative values have been neglected to provide a focus on areas with population growth.

The impact of climate change on photovoltaic performance can be estimated in a number of different ways. We compare and discuss the following four scenarios:

Scenario 0 – Naïve estimate

A simplistic estimate can be obtained by taking the global average temperature increase and multiply it with the tabulated temperature coefficient of a solar cell. This scenario makes no assumptions about the distribution of solar cells on the planet or correlations between parameters. For the naïve estimate, we use the average temperature data for the RCP4.5 scenario from [53], and tabulated temperature coefficient values for silicon (-0.45%/K) and CdTe (-0.26%/K).

Scenario 1 – PV everywhere

In a first detailed scenario we use distributed temperature changes around the globe, and we assume that solar panels are installed uniformly on all land masses around the planet. A uniform distribution makes no assumption about installation strategies and requires a pervasive grid to allow free transportation of electricity. For all detailed scenarios we use implied temperature coefficients for silicon (-0.52%/K) from **Figure 7** and tabulated values for CdTe (-0.26%/K). By using the implied temperature coefficient, we make the assumption that temperature, precipitable water and aerosols will develop in a way that is consistent with the development observed in the covered ten-year period. It should be noted that, while trends are consistent with longer term observations, this may not be the case.

Scenario 2 – Where the people are

The second detailed scenario assumes that solar cell capacity is installed proportionally to the population density in an area. Population development until 2100 is projected based on the Shared Socioeconomic Pathways (SSP) "Middle of the Road" scenario (SSP2) [51, 52]. Data were obtained from NASAs Socioeconomic Data and Applications Center (SEDAC) [54]. Population distribution as well as total global population are shown in **Figure 5b**. This scenario can be interpreted as a minimum infrastructure scenario in which transport distance for electricity is reduced.

Scenario 3 – Where the sun is

The third detailed scenario assumes that solar cell capacity is installed proportionally to solar insolation on land. Average insolation for the covered ten-year time period was used for global distribution. This scenario can be interpreted as a strategy to reduce the number of solar panels needed by placing them more frequently in very sunny areas.

Projections for all scenarios and the different solar cell technologies are displayed in **Figure 11**. Detailed scenarios are rendered in color (blue for silicon, green for CdTe), the naïve scenario in greyscale (black for silicon, grey for CdTe). The shaded areas, and the bars in the rightmost figure, correspond to the range given by the RCP2.6 (lower limit) and the RCP8.5 (upper limit) climate scenario [53].

The detailed scenarios predict a reduction in solar cell performance that is significantly higher than the naïve scenarios (1.3% vs. 0.75% for silicon in RCP4.5). The main contributor to this difference is the fact that the detailed scenarios only consider changes in temperature above land masses. A second contributor is the slightly higher implied temperature coefficient from the correlation analysis compared to the tabulated value (-0.52%/K vs -0.45%/K).

It is noteworthy that projected values mark global averages, and extreme values can be significantly higher. Specifically, the detailed scenarios projects reductions that are twice as high as the average and

more, for example, in the Southwest of the United States, parts of Eastern Europe and western Asia. Furthermore, it should be noted that the presented results neglect diurnal variations. Many climate models show that temperatures during the night rise more than during the day (see for example [55]). Differences between ΔT_{min} and ΔT_{max} on the order of 0.12K over a period of 50 years were reported there.

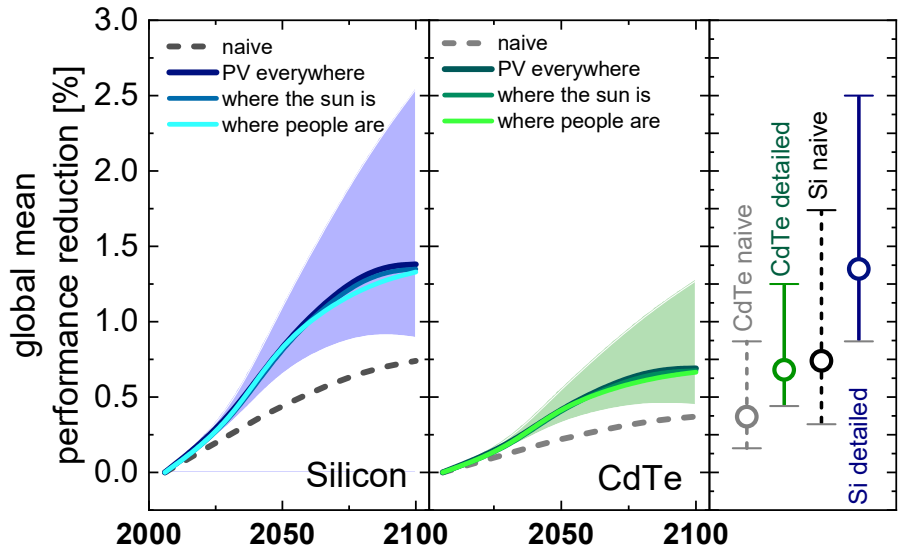

Figure 11: *Projected reduction in solar cell performance. In the leftmost part of the figure results for silicon (blue) are shown compared to the naïve baseline (black dashes). The middle part of the figure shows the same for CdTe (green and grey dashes). Lines correspond to the RCP 4.5 global warming scenario, shaded areas and bars in the rightmost figure mark the range of results for different IPCC projection (lower limit —RCP2.6, upper limit — RCP8.5).*

Discussion:

- **It's already happening:**

  The signatures of climate change and global warming are already affecting solar cells and we should already be able to detect them on solar cell performance. **Figure 4b** shows that the median

performance reduction of silicon solar cells around the planet in the recent past has been on the order of -0.04% relative per year, with reduction of more than twice that value not being uncommon. The average reduction is about one tenth that of the technologies power degradation rate [29] and should be noticeable on the ten-year timescale that this study was conducted on. The effect should be especially noticeable in regions in which temperature changes were more pronounced like Spain or the Northwestern United States. In addition, solar cells are detectors and solar farms use additional detectors to map local meteorological conditions. Data from these installations could help to more precisely record the effects of climate change and better understand its impact.

- **Technology matters:**

  In this study we have considered two solar cell technologies, Si and CdTe that feature different band gaps and exhibit different sensitivities to changing climate conditions (**Figures 3** and **4**). Materials with a higher band gap (ideally 1.3 eV and above) show greater robustness to variations in temperature and humidity than lower band gap materials [13], but are more sensitive to aerosols. Screening for new PV materials [44], as well as optimizing current PV materials and modules [45] should take these considerations into account.

  Performance can also be improved within established PV technologies. As solar cell efficiencies increase, less of the absorbed light is turned into heat, resulting in overall lower operating temperatures of the module [58]. Module- and cell architectures can also help to reduce sensitivities to temperature. For example, [10] reports temperature coefficients as low as -0.3%/K for a bifacial PV module with *n*-type crystalline Si heterojunction solar cells. It can be expected that temperature related performance reductions will be smaller in the future.

- **It's not all about cell performance:**

  In this study we concentrated on the fundamental and intrinsic effects of global warming on solar cells, yet solar installations will be affected in other, and quite likely more significant ways - particularly through degradation and through more extreme weather events.

  In 2012, Jordan *et al.* at NREL conducted a study about how degradation correlates with climatic conditions [59]. Humidity and temperature are stated to be undoubtedly relevant for PV performance. Correspondingly, Si as well as thin-film PV modules were found to degrade faster in hot and humid climates. Degradation does not only affect the solar cell, but the PV module as a whole. Gagliardi *et al.* [60], for example, projected the long-term degradation of EVA globally as a function of climate zones and underlined the role of humidity. Moisture ingress is also one cause for corrosion of the metallic silver grid [61]. All these results are indications that the observed trends in climate development will lead to higher degradation rates in all PV module types. Additional performance reduction through faster degradation is likely to be more significant than that caused by elevated junction temperatures.

  Climate change also results in an increased frequency of higher impact extreme weather events. While solar farms generally stand up well to high winds, flooding or hail [62], extreme weather events like Hurricanes can be problematic. A report from the Rocky Mountain institute [63] analysed solar installations in the Caribbean after hurricanes Harvey, Irma, and Maria and found that, while many survived, some installations were severely damaged. Weather events do not affect performance in the same way as junction temperatures, but are likely to cause considerable economic damage.

  An additional factor to consider is air pollution [30, 64]. Globally, air pollution levels are raising — especially in China and India, among the largest installers in PV — yet Europe and the US have successfully reduced overall particle concentrations [65]. Yield reductions will have to be adjusted for increasing air pollution levels, especially for materials with higher band gaps, as **Figure 9** indicates.

- **Deployment strategies could help:**

  Figure 11 shows that there is a difference in performance reduction depending on how solar panels are distributed around the world. Scenarios 2 and 3 both show slightly smaller losses than the PV everywhere scenario. While a more developed grid has only small implication on the average reduction, it will help manage larger variations in between regions. A more developed grid will support PV deployment in general, as it enables more flexibility in choosing installation sites and in shifting generation between locations. Results from a study by the American Physical Society suggest that new approaches to extend and operate the grid will be required with 30% electricity generation from renewable sources [66]. Other advantages of advanced grids are pointed out, *e.g.,* in [67].

- **It will cost us:**

  In the RCP8.5 scenario, PV electricity production could be reduced by more than 2.5% on average by 2100 with local performance reductions exceeding twice this value, compared to a 2010 baseline. Many communities today have defined targets for high renewable energy contributions to electricity demands [68]. At the same time, it is believed that our energy needs will more than double by the end of the century [69]. To supply half the world electricity demand by 2100 with PV would require a capacity in the range of 15 to 20 TW [70]. A 2% performance reduction would then equal 300 to 400 GW_P in capacity. For comparison, 400 GW_P in capacity were installed globally cumulatively by the end of 2017 [71] or to, in terms of electricity production, roughly the total electricity generation of Germany today or to, in terms of dollar value, on the order of 100s of billion USD in today's value of PV systems. Furthermore, faster degradation and more extreme weather events are likely to reduce the average lifetime of a PV system, an effect that could very well exceed the 2% mark on overall performance reduction, and could exceed it substantially, in addition to raising costs for insurances [72].

We have chosen in this discussion deployment numbers that are high but not inconceivable. Yet, even if only a fraction of the assumed PV capacity is installed, and even if global warming is limited to 1.5C by the end of the century, raising temperatures will cause economic damage to PV installations that is significant. An effect with a magnitude of 1% may appear small, but as renewable energies become a major contributor to our energy infrastructure, small effects start to matter.

Summary:

Solar cells are sensitive to the conditions under which they operate, particularly to temperature, humidity and aerosols. A changing climate has an effect on PV power generation. In this paper, we presented our findings obtained through statistical analysis of satellite measured meteorological data and modeled photovoltaic field performance. The analysis was carried out in four steps:

Step 1: We analyzed trends in relevant operating conditions for solar cells in the ten-year period between 2006 and 2015. Operating conditions considered include changes in insolation, temperature, and precipitable water and aerosol related light transmission through the atmosphere (**Figure 2**). The analysis confirmed an overall global rising temperature and an increase in total precipitable water, resulting in a reduced light transmission through the atmosphere.

Step 2: We repeated the analysis for global energy yield (**Figure 3**) and performance ratio (**Figure 4**) data of Si and CdTe solar cells data, using calculations based on a field-validated performance model. We found that energy yield for the reference silicon and CdTe PV modules has already decreased by 0.4 kWh/ year and 0.1 kWh/ year, respectively. While overall small, the effect on performance ratio for silicon is -0.04%/year, about one tenth of the technologies degradation rates, these effects are large enough an dit should be possible to measure them.

Step 3: We analyzed the correlations between trends in meteorological and solar cell performance parameters. We used a cluster analysis to identify six types of areas with different characteristics of recent climate change. Clustering assists the correlation analysis by providing an explanation for shifts and

outliers. We found that temperature is the leading factor to affect performance of silicon solar cells, and accounts for about 85% of the observed effect (**Figure 7a**). While less explicit, we found indications that the majority of the remaining effect can be attributed to changes in precipitable water (**Figure 8a** and supporting material). The situation for CdTe is less clear because it is partially masked by spectral effects that result in unintuitive behavior of the calculated performance ratio. Raising temperatures still result in a reduction in CdTe performance ratio, yet at a rate that is smaller than expected (**Figure 7b**). The reason lies in the signature of precipitable water. Because CdTe is largely not affected by water related light absorption, performance ratio increases with higher atmospheric water contents (**Figure 8b**), a quirk of the procedure for calculating the metric. The same effect results in a clear signature of aerosols (**Figure 9**).

Step 4: We used the established correlations to project the future performance of photovoltaic installations according to IPCC climate scenarios. Given the challenges of predicting future insolation, we focus on the implications of changes in temperature. For this purpose, we calculate changes in performance ratio using the implied temperature coefficient from **Figure 7a** for silicon and tabulated values for CdTe. Using an implied temperature coefficient, we implicitly consider the added effect of humidity and aerosols. Depending on the climate change scenario, we project relative decreases for silicon PV panels by 2100 between approx. 0.7% and 2.5% (**Figure 11**), translating to 8 – 30 kWh/kWp in North America. An additional finding in this step is that the magnitude of this decrease depends not only on global warming but also on technology. This finding highlights the benefits of developing more robust absorber materials or device architectures.

Beyond the fundamental effects on solar cell performance analyzed here, climate change may pose additional challenges, for example by accelerating PV module degradation through heat and water ingress. And the implications go further still: the projected losses will be intensified by the development of air quality. Regions in which dust and pollution increase will see much higher losses than projected here. The combined performance penalties will have a considerable socio-economic impact, especially if

solar energy becomes a leading contributor to satisfying the world's raising electricity demands. Solar panels produced today may well generate electricity for the next 50 years [73], making it necessary to develop strategies to accommodate for these issues now. The right technology and the right design can not only help to reduce global warming [74], but also provide stability in a changing environment.

Acknowledgment:

Climate scenarios used were from the NEX-GDDP dataset, prepared by the Climate Analytics Group and NASA Ames Research Center using the NASA Earth Exchange, and distributed by the NASA Center for Climate Simulation (NCCS). Insolation data were obtained from the NASA Langley Research Center Atmospheric Science Data Center. This work was financially supported by the DOE-NSF ERF for Quantum Energy and Sustainable Solar Technologies (QESST) and by funding from Singapore's National Research Foundation through the Singapore MIT Alliance for Research and Technology's "Low energy electronic systems (LEES) IRG"

Data Availability Statement:

Insolation data used in this study is available via NASA's Clouds and the Earth's Radiant Energy System (CERES) website https://ceres.larc.nasa.gov/products.php?product=SYN1deg (registration required). Data can be ordered via the Atmospheric Science Data Center (ASDC) https://eosweb.larc.nasa.gov/project/ceres/syn1deg_table. Temperature, humidity and aerosol data are available from NASA's EARTHDATA website https://search.earthdata.nasa.gov. Temperature and Humidity data using the data set entitled: AIRS/Aqua L3 Daily Standard Physical Retrieval (AIRS-only) 1 degree x 1 degree V006 (AIRS3STD) at GES DISC, aerosol data using OMI/Aura Near UV Aerosol Optical Depth and Single Scattering Albedo L3 1 day 1.0 degree x 1.0 degree V3 (OMAERUVd) at GES DISC (single Scattering Albedo) and MODIS/Terra Aerosol Cloud Water Vapor Ozone Daily L3 Global 1Deg CMG (AOD and Angstrom parameter). Population data is available via NASAS's Socioeconomic Data and Applications

Center (SEDAC) via http://sedac.ciesin.columbia.edu/data/set/popdynamics-pop-projection-ssp-2010-2100. Global warming data (RCP4.5) is available from the International Institute for Applied Systems Analysis (IIASA) website http://www.iiasa.ac.at/web-apps/tnt/RcpDb/dsd?Action=htmlpage&page=about (registration required).

Code Availability Statement:

The codes used for this analysis were implemented in Mathematic (version 11.2) and are available without restriction upon request to impeters@mit.edu.

Supporting Material:

Trends in precipitable water and aerosol optical depth

In **Figure 2c** and **d,** we show the trends in water related- and aerosol related light transmission through the atmosphere. For the sake of completeness, we have added the annual changes in precipitable water and aerosol optical depth here (**Figure S1**). Qualitatively, the graphs show the same trend, yet as a metric and to establish correlations, light transmission is a more meaningful parameter. Light transmission not only depends on the change, but also on the baseline value for each location

a) annual change in Total Precipitable Water b) annual change in AOD

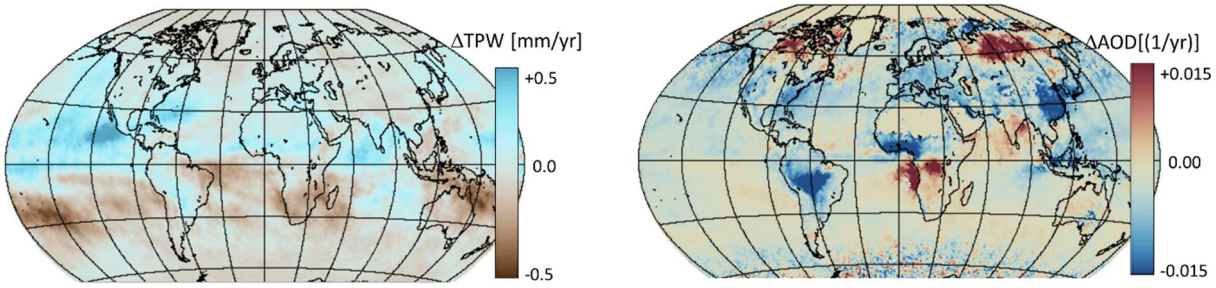

Figure S1: M*aps of the average annual changes in total precipitable water ΔTPW (a) and aerosol optical depth (AOD) ΔAOD (b). These maps were used to calculate the corresponding changes in light transmission as shown in Figure 2.*

Correlation between changes in meteorological parameters:

Correlation between the changes in meteorological parameters over time reveal synergies in the observed development of energy yield and performance ratios. In **Figure S2** the values for the four considered meteorological parameters are plotted against each other with additional color coding used to show how values distribute over latitude. The black line is the linear fit of this data.

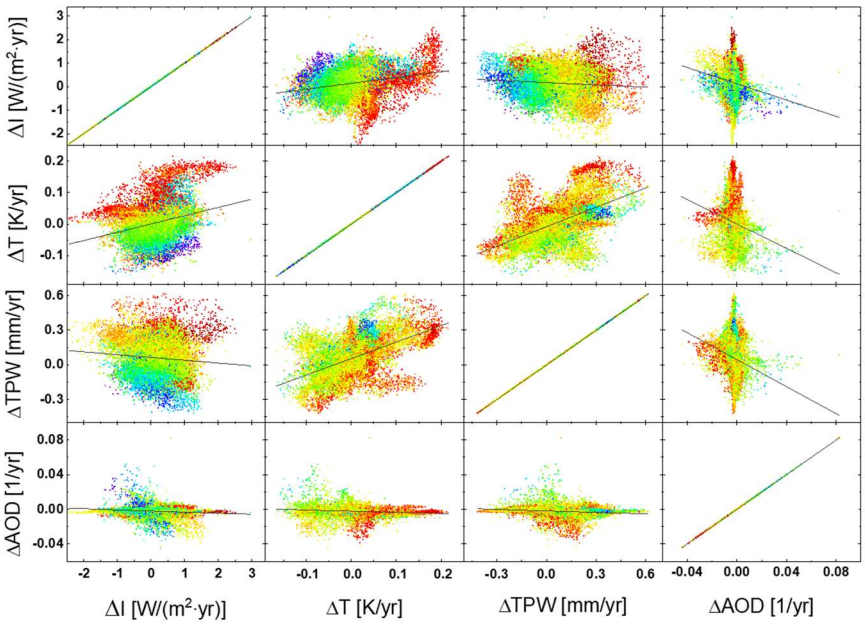

Figure S2: *correlation matrix for the annual development of the four considered meteorological parameters insolation (I), temperature (T), total precipitable water (TPW) and atmospheric optical depth (AOD) as shown in Figure 2 and Figure S1. Colors indicate different latitudes.*

We have calculated the Pearson correlation for the data clouds shown in **Figure S2** and summarized the results in a matrix:

$$\begin{pmatrix} 1 & 0.26 & -0.09 & -0.15 \\ 0.26 & 1 & \mathbf{0.54} & -0.16 \\ -0.09 & \mathbf{0.54} & 1 & -0.18 \\ -0.15 & -0.16 & -0.18 & 1 \end{pmatrix}$$

We find a moderate to strong positive correlation (0.54) between changes in temperature and changes in total precipitable water, indicating that in general areas that get warmer also tend to get more humid. Additionally, there is a moderate to small positive correlation (0.26) between temperature and insolation, indicating that some of the temperature development is due to variations in the amount of sunlight received. The remaining pairings all show weak negative correlations

Statistical distribution of changes in meteorological parameters:

We have also analyzed the statistical distribution of ten changes in the four considered meteorological parameters based on the ten years between 2006 and 2015. The histograms are shown in **Figure S3**.

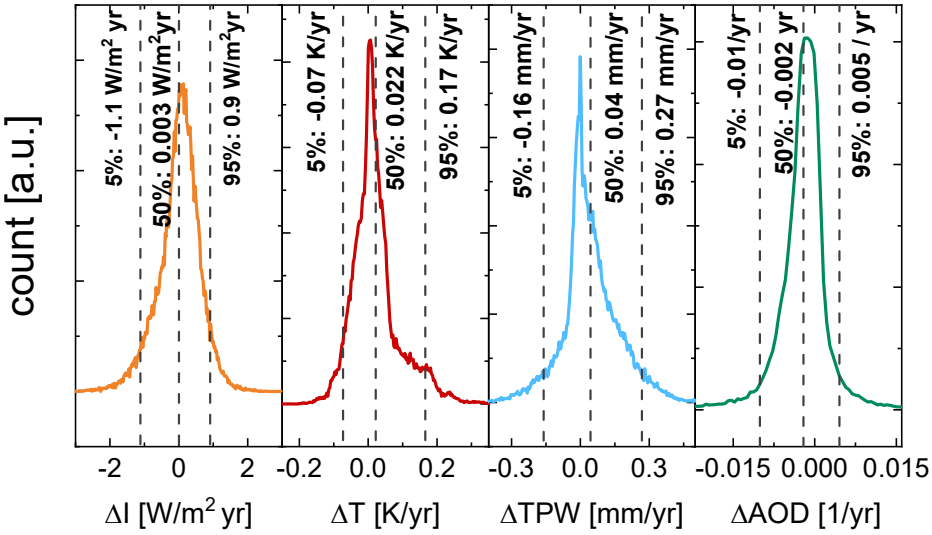

Figure S3: *Statistical distribution of annual changes in insolation (I), temperature (T), total precipitable water (TPW) and aerosol optical depth (AOD) as shown in Figure 2.*

As expected, insolation does on average not change. Yet some areas receive an increasing- and some areas a decreasing amount of sunlight due to statistical variations over the considered period. For temperature, we find an increase of on average of 0.02 K/year, which is consistent with global land and ocean warming rates observed over the past forty years [75]. It is well established that an increase in temperature coincides with an increase in humidity (see for example [76]) and trends found here (0.04 mm/year on average increase in total precipitable water) are in line with results found in literature (see for example [77]).

Temperature and PR trends for the different clusters

Figure 7 shows the aggregated analysis for the correlation of temperature changes and performance ratio changes. To expand on this, here we provide the correlation analysis for each cluster (**Figure S4**). For silicon, it can be observed that, per trend the temperature coefficient increases with temperature. For CdTe, no clear trends are visible.

a) Silicon b) CdTe

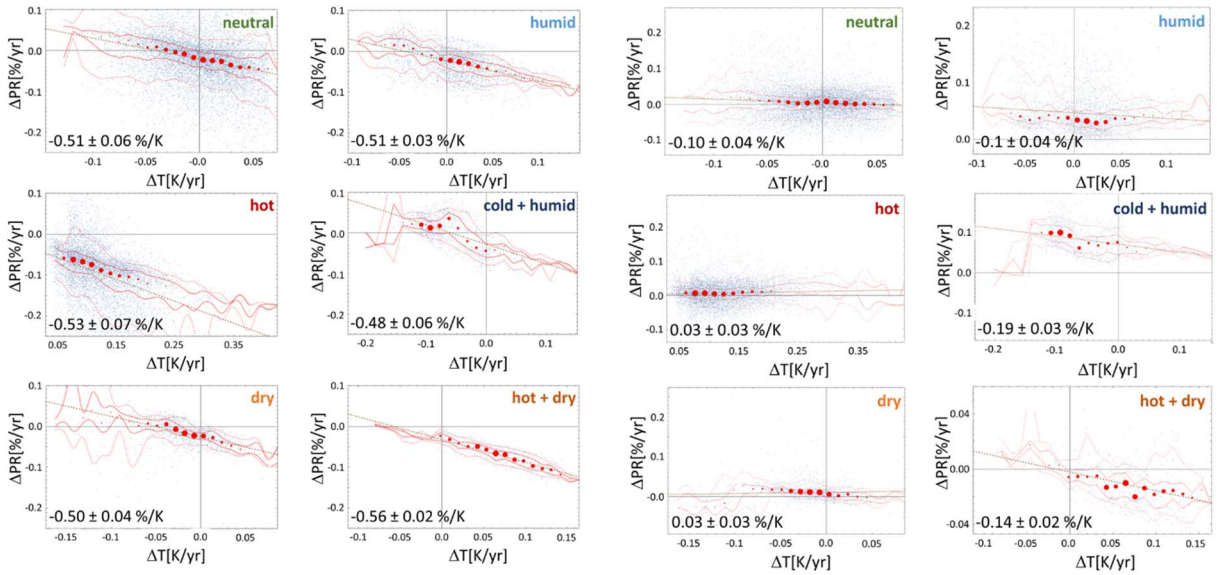

Figure S4: *ΔPR plotted against ΔT for the different clusters for silicon (a) and CdTe (b). The red dots mark the median value in ΔT bins, dots size indicates the number of points in each bin. The lines mark, from bottom to top, the 5-, 30-, 50-, 70- and 95-percentile of each dataset.*

Eliminating the influence of humidity.

To investigate the influence of precipitable water on the implied temperature coefficient in **Figure 7a**, we filtered the available data for conditions with a negligible change in total precipitable water. For this purpose, we only considered data points within a small interval around 0 on the x-axis in **Figure S5a**. Using this filtered data, we obtain an implied temperature coefficient of TCI = -0.48 ± 0.06%/K. This result is

taken as an indication that precipitable water may be responsible for the discrepancy between the implied and the tabulated temperature coefficient.

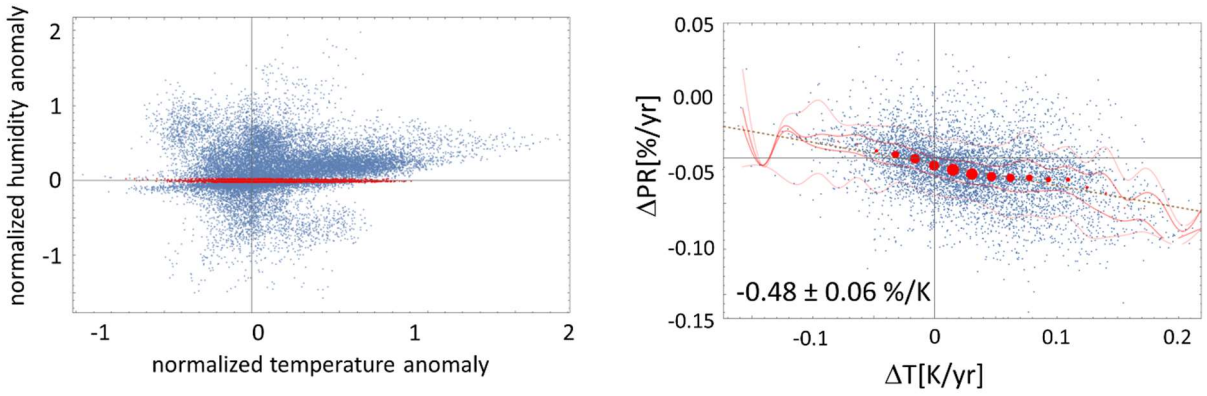

Figure S5: *Filtering for conditions with minimal influence of precipitable water changes (a). The filtered data is used to calculate an implied temperature coefficient (b). The exercise was repeated for various intervals around 0, with no significant changes to the result.*

References:

[1] IPCC, 2014: Climate Change 2014: Synthesis Report. Contribution of Working Groups I, II and III to the Fifth Assessment Report of the Intergovernmental Panel on Climate Change [Core Writing Team, R.K. Pachauri and L.A. Meyer (eds.)]. IPCC, Geneva, Switzerland, 151 pp.

[2] IEA, Market Report Series: Renewables 2017, ISBN 978-92-64-28187-5.

[3] BP Energy Outlook 2018 Edition, https://www.bp.com/en/global/corporate/energy-economics/energy-outlook.html

[4] N. M. Haegel, R. Margolis, T. Buonassisi, D. Feldman, A. Froitzheim, R. Garabedian, M. Green, S. Glunz, H.-M. Henning, B. Holder, I. Kaizuka, B. Kroposki, K. Matsubara, S. Niki, K. Sakurai, R. A. Schindler, W. Tumas, E. R. Weber, G. Wilson, M. Woodhouse, S. Kurtz, Terawatt-scale photovoltaics: Trajectories and challenges, Science, 356 (2017), 141 – 143.

[5] https://www.nrel.gov/pv/cell-efficiency.html

[6] A comprehensive summary of learning curves for module cost, energy and material demand for production and energy payback time is given in the Photovoltaics Report prepare by Fraunhofer ISE. The report can be downloaded from: https://www.ise.fraunhofer.de/content/dam/ise/de/documents/publications/studies/Photovoltaics-Report.pdf

[7] https://www.greentechmedia.com/articles/read/140-gigawatts-of-solar-and-wind-capacity-added-in-2018-irena-says#gs.gwz4i7

[8] N. Haegel et al., Terawatt-scale photovoltaics: Transform global energy, Science 364:6443 (2019), 836-838.

[9] P. Würfel, The chemical potential of radiation, Journal of Physics C: Solid State Physics,15: 18 (1982), 3967-3985.

Scientific studies about temperature coefficients for silicon include:

[10] J. Lopez-Garcia, D. Pavanello, T. Sample, Analysis of Temperature Coefficients of Bifacial Crystalline Silicon PV Modules, IEEE Journal of Photovoltaics, 8:4 (2018), 960 – 968.

[11] S Ponce-Alcántara, J. P. Connolly, G. Sánchez, J. M. Míguez, V. Hoffmann, R. Ordás A statistical analysis of the temperature coefficients of industrial silicon solar cells. Energy Procedia 55 (2014) 578 – 588.

Manufacturer ratings are given, for example, in:

[12] https://blog.pickmysolar.com/does-solar-panel-temperature-coefficient-matter

[13] M. Peters, T. Buonassisi, Energy Yield Limits for Single Junction Solar Cells, Joule 2 (2018), 1160 -1170.

[14] A. M. Nobre, S. Karthik, H. Liu, D. Yang, F. R. Martins, E. B. Pereira, R. Rüther, T.Reindl, I. M. Peters, On the impact of haze on the yield of photovoltaic systems in Singapore, Renewable Energy, 89 (2016), 389 – 400.

[15] R. Saeger, N. Naik and G. A. Vecchi, Thermodynamic and Dynamic Mechanisms for Large-Scale Changes in the Hydrological Cycle in Response to Global Warming, Journal of Climate, 23 (2010), 4651 – 4668.

[16] J. A. Crook, L. A. Jones, P. M. Forstera and R. Crook, Climate change impacts on future photovoltaic and concentrated solar power energy output, Energy Environ. Sci., 2011, 4, 3101–3109.

[17] Climate Change 2007 - The Physical Science Basis Contribution of Working Group I to the Fourth Assessment Report of the IPCC (ISBN 978 0521 88009-1 Hardback; 978 0521 70596-7 Paperback).

[18] Wild M, Folini D, Henschel F, Fischer N, Muller B (2015) Projections of long-term changes in solar radiation based on CMIP5 climate models and their influence on energy yields of photovoltaic systems. Sol Energ 116: 12-24.

[19] IPCC, 2013: Climate Change 2013: The Physical Science Basis. Contribution of Working Group I to the Fifth Assessment Report of the Intergovernmental Panel on Climate Change [Stocker, T.F., D. Qin, G.-K. Plattner, M. Tignor, S.K. Allen, J. Boschung, A. Nauels, Y. Xia, V. Bex and P.M. Midgley (eds.)]. Cambridge University Press, Cambridge, United Kingdom and New York, NY, USA, 1535 pp.

[20] S. Jerez, I. Tobin, R. Vautard, J. P. Montavez, J. M. Lppez-Romero, F. Thais, B. Bartok, O. Bøssing Christensen, A. Colette, M. Deque, G. Nikulin, S. Kotlarski, E. van Meijgaard, C. Teichmann, & M. Wild, The impact of climate change on photovoltaic power generation in Europe, Nature Communications (2015), DOI: 10.1038/ncomms10014.

[21] S. D. Bazyomo, E. A. Lawin, and A. Ouedraogo, Seasonal Trends in Solar Radiation Available at the Earth's Surface and Implication of Future Annual Power Outputs Changes on the Photovoltaic Systems with One and Two Tracking Axes, J Climatol Weather Forecasting 2017, 5:1, DOI: 10.4172/2332-2594.1000201.

[22] N. H. Reich, B. Mueller, A. Armbruster, W. G. J. H. M. van Sark, K. Kiefer, C. Reise, Performance ratio revisited: is PR > 90% realistic?, Progress in Photovoltaics: Research and Applications, 20:6 (2012), 717-726.

[23] K. Kajiwara, T.Oozeki, Y. Genchi, Effect of Temperature on PV Potential in the World, Environ. Sci. Technol. 45 (2011), 9030–9035.

[24] M. D. Bartos, M. V. Chester, Impacts of climate change on electric power supply in the Western United States, Nature Climate Change, 5 (2015).

[25] M. Peters, H. Liu, T. Reindl, T. Buonassisi, Global prediction of photovoltaic field performance differences using open-source satellite data, Joule 2 (2018), 307 – 322.

[26] O. Dupré, R. Vaillon, M.A. Green, Physics of the temperature coefficients of solar cells, Solar Energy Materials and Solar Cells, 140 (2015), 92 – 100.

[27] Y. Tsunomura, Y. Yoshimine, M. Taguchi, T. Baba, T. Kinoshita, H. Kanno, H. Sakata, E. Maruyama, M.Tanaka, Twenty-two percent efficiency HIT solar cell, Solar Energy Materials and Solar Cells, 93: 6–7 (2009), 670-673.

[28] http://www.firstsolar.com/-/media/First-Solar/Technical-Documents/Series-4-Datasheets/Series-4V2-Datasheet.ashx

[29] A. Fell, et al. Input Parameters for the Simulation of Silicon Solar Cells in 2014, IEEE JPV, 5 (2015), 1250 -1263.

[30] M. Peters, S. Karthik, H. Liu, T. Buonassisi, A. Nobre, Urban Haze and Photovoltaics, Energy Environ. Sci., 11 (2018), 3043-3054.

[31] V.M. Velasco Herrera, B. Mendoza, G. Velasco Herrera, Reconstruction and prediction of the total solar irradiance: From the Medieval Warm Period to the 21st century, New Astronomy 34 (2015) 221–233.

[32] https://ceres.larc.nasa.gov/

[33] AIRS Science Team/Joao Texeira (2013), AIRS/Aqua L3 Daily Standard Physical Retrieval (AIRS-only) 1 degree x 1 degree V006, Greenbelt, MD, USA, Goddard Earth Sciences Data and Information Services Center (GES DISC), Accessed: [10/25/2018], doi:10.5067/Aqua/AIRS/DATA303

[34] http://www.nasa.gov/mission_pages/aura/spacecraft/omi.html

[35] https://modis.gsfc.nasa.gov/

[36] Gueymard, C.A. SMARTS, “A Simple Model of the Atmospheric Radiative Transfer of Sunshine: Algorithms and Performance Assessment”. Professional Paper FSEC-PF-270-95. Florida Solar Energy Center, 1679 Clearlake Rd., Cocoa, FL 32922 (1995).

[37] Gueymard, C. A. "Parameterized Transmittance Model for Direct Beam and Circumsolar Spectral Irradiance." Solar Energy 71:5 (2001), 325-346.

[38] STC for terrestrial solar cells refer to tests done at 1000 W/m2 irradiance, a temperature of 25˚C and at a solar spectrum, referred to as the AM1.5 spectrum and specified by the ASTM-G173 standard (https://www.astm.org/Standards/G173.htm).

[39] Fraunhofer Institute for Solar Energy Systems, ISE, Photovoltaic Status Report, presented Freiburg, 19 June 2018, https://www.ise.fraunhofer.de/en/publications/studies/photovoltaics-report.html

[40] Pearson, K., Notes on regression and inheritance in the case of two parents, Proceedings of the Royal Society of London, 58 (1895), 240–242.

[41] https://earthobservatory.nasa.gov/WorldOfChange/decadaltemp.php

[42] NASA's Goddard Institute for Space Studies (GISS), https://climate.nasa.gov/vital-signs/global-temperature/

[43] Hansen, J., R. Ruedy, M. Sato, and K. Lo (2010), Global surface temperature change, Rev. Geophys., 48, RG4004, doi:10.1029/2010RG000345.

[44] Borisenkov, Y. P., Tsvetkov, A. V., Eddy, J. A. , Combined Effects of Earth Orbit Perturbations and Solar Activity on Terrestrial Insolation. Part I: Sample Days and Annual Mean Values, Journal of the Atmospheric Sciences, 42:9 (1985), 933 – 940.

[45] Haurwitz, B., Insolation in relation to cloudiness and cloud density, J. Meteor., 2 (1945), 154–166.

[46] Simpson, E. H. "The Interpretation of Interaction in Contingency Tables". Journal of the Royal Statistical Society, Series B. 13 (1951), 238–241.

[47] Specifics about the method can be found in the tutorials of Mathematica (https://reference.wolfram.com/language/tutorial/PartitioningDataIntoClusters.html), a general description of contraction algorithms is provided, for example, in D. Karger, C. Stein, A New Approach to the Minimum Cut Problem, Journal of the ACM, 43:4, (1996), 601 - 640.

[48] M. A. Green, General temperature dependence of solar cell performance and implications for device modelling. Progress in Photovoltaics: Research and Applications, 11 (2003), 333-340.

[49] M. Meinshausen, S. J. Smith, K. Calvin, J. S. Daniel, M. L. T. Kainuma, J-F. Lamarque, K. Matsumoto, S. A. Montzka, S. C. B. Raper, K. Riahi, A. Thomson, G. J. M. Velders, D.P. P. van Vuuren, The RCP greenhouse gas concentrations and their extensions from 1765 to 2300. Climatic Change, 109 (2011), 213 - 241.

[50] B. Thrasher, E. P. Maurer, C. McKellar, & P. B. Duffy Technical Note: Bias correcting climate model simulated daily temperature extremes with quantile mapping. Hydrology and Earth System Sciences, 16 (2012), 3309-3314.

[51] B. Jones, B. C. O'Neill. 2017. Global Population Projection Grids Based on Shared Socioeconomic Pathways (SSPs), 2010-2100. Palisades, NY: NASA Socioeconomic Data and Applications Center (SEDAC). https://doi.org/10.7927/H4RF5S0P. Accessed 28th July 2018.

[52] B. Jones, B. C. O'Neill. 2016. Spatially Explicit Global Population Scenarios Consistent with the Shared Socioeconomic Pathways. Environmental Research Letters, 11 (2016): 084003. https://doi.org/10.1088/1748-9326/11/8/084003.

[53] Reto Knutti and Jan Sedlacek. "Robustness and uncertainties in the new CMIP5 climate model projections". In: Nature Climate Change 3.4 (2012), 369–373.

[54] http://sedac.ciesin.columbia.edu/data/set/popdynamics-pop-projection-ssp-2010-2100.

[55] K. Braganza, D. J. Karoly, J. M. Arblaster, Diurnal temperature range as an index of global climate change during the twentieth century, Geophysical Research Letters, 31:13 (2004), L13217.

[56] R. E. Brandt et al., Searching for "defect-tolerant" photovoltaic materials: Combined theoretical and experimental screening, *Chemistry of Materials* **29**, 4667–4674 (2017).

[57] According to the International Roadmap for Photovoltaic (ITRPV) 9th edition, 2018, PV panel prices by the end of 2017 had dropped as low as 0.34$/W.

[58] Skoplaki, E., and Palyvos, J.A., Operating temperature of photovoltaic modules: a survey of pertinent correlations. Renew. Energy 34 (2009), 23–29.

[59] D. C. Jordan, J. H. Wohlgemuth, and S. R. Kurtz, Technology and Climate Trends in PV module Degradation, Presented at the 27th European Photovoltaic Solar Energy Conference and Exhibition Frankfurt, Germany September 24–28, 2012.

[60] M. Gagliardi, M. Paggi, Long-term EVA degradation simulation: Climatic zones comparison and possible revision of accelerated tests, Solar Energy 159 (2018) 882–897.

[61] I. Duerr, J. Bierbaum, J. Metzger, J. Richter, D. Philipp, Silver Grid Finger Corrosion on Snail Track affected PV Modules – Investigation on Degradation Products and Mechanisms, Energy Procedia 98 (2016), 74-85.

[62] V. Fthenakis, The resilience of PV during natural disasters: The hurricane Sandy case, proceedings 39th IEEE Photovoltaic Specialists Conference (PVSC), 2014, 10.1109/PVSC.2013.6744949.

[63] C. Burgess, J. Goodman, Solar Under Storm (2018), https://rmi.org/wp-content/uploads/2018/06/Islands_SolarUnderStorm_Report_digitalJune122018.pdf.

[64] M. Wild, Global dimming and brightening: a review. J. Geophys. Res. – Atmos. 114 (2009), D00D16.

[65] E. W. Butt, S. T. Turnock, R. Rigby, C. L. Reddington, M. Yoshioka, J. S. Johnson, L. A. Regayre, K. J. Pringle, G. W. Mann and D. V. Spracklen, Global and regional trends in particulate air pollution and attributable health burden over the past 50 years, Environ. Res. Lett. 12 (2017) 104017.

[66] APS Panel of Public Affairs, Integrating Renewable Electricity on the Grid (2010).

[67] Cedric Clastres, Smart grids: Another step towards competition, energy security and climate change objectives, Energy Policy, 39 (2011), 5399–5408.

[68] As of June 2019 there are numerous examples of countries, states, cities and organizations that have made a pledge for 100% carbon free electricity. One example tat has attracted considerable attention is California: https://www.latimes.com/business/la-fi-100-percent-clean-energy-20190110-story.html.

[69] Jason Deign, Global Energy Demand Could Grow 124% by 2100: Even Fossil Fuels Won't Cut It, Greentech Media, February 2nd 2018, https://www.greentechmedia.com/articles/read/energy-needs-in-2100-even-fossil-fuels-will-not-cut-it#gs.hsqdgs.

[70] One example for an outlook on PV deployment development is F. Creutzig, P. Agoston, J. C. Goldschmidt, G. Luderer, G. Nemet, and R. C. Pietzcker, "The underestimated potential of solar energy to mitigate climate change", 2, 17140 (2017). A back of the envelope calculation is: the current world electricity demand is 21000TWh / year, assuming a 125% growth by 2100, results in a total need of 47000TWh. With a specific yield of 1500kWh/kWp, 15TW of installed PV capacity would contribute 50% of this demand.

[71] International Energy Agency, A Snapshot of Global PV (1992 - 2017), ISBN 978-3-906042-72-5.

[72] D. Grossman, Global Warming Is Already Costing the Insurance Industry Historic Amounts, Popular Mechanics, Apr 17, 2019.

[73] V. Poule, D.S. Strebkov, I.S. Persic, M. Libra, Towards 50 years lifetime of PV panels laminated with silicone gel technology. Solar Energy 86 (2012), 3103–3108.

[74] D. Berney-Needleman, J. R. Poindexter, R. C. Kurchin, I. M. Peters, G. Wilson, T. Buonassisi, Economically sustainable scaling of photovoltaics to meet climate targets, Energy & Environmental Science, 9 (2016), 2122-2129.

References in the supporting material

[75] NASA's Goddard Institute for Space Studies (GISS), https://climate.nasa.gov/vital-signs/global-temperature/

[76] Wagner, T., S. Beirle, M. Grzegorski, and U. Platt, Global trends (1996–2003) of total column precipitable water observed by Global Ozone Monitoring Experiment (GOME) on ERS-2 and their relation to near-surface temperature, J. Geophys. Res., 111 (2006).

[77] Roman, J., R. Knuteson, S. Ackerman, and H. Revercomb, 2015: Predicted Changes in the Frequency of Extreme Precipitable Water Vapor Events. J. Climate, 28, 7057–7070 (2015).